



ORIGINAL ARTICLE

Relationship between the performance of pervious concrete slabs with steel slag and the shape properties of coarse aggregates

Relação entre a performance de placas de concreto permeável com escória de aciaria e as propriedades de forma de agregados graúdos

Helano Wilson Pimentel^a Ivo de Castro Carvalho^b Webert Brasil Cirilo da Silva^{c,d} André Rocha Chaves^b Lucas Feitosa de Albuquerque Lima Babadopulos^b

^aUniversidade Federal do Ceará – UFC, Programa de Pós-graduação em Engenharia e Ciência de Materiais, Departamento de Engenharia Metalúrgica e de Materiais, Fortaleza, CE, Brasil

^bUniversidade Federal do Ceará – UFC, Programa de Pós-graduação em Engenharia Civil: Estruturas e Construção Civil, Departamento de Engenharia Estrutural e Construção Civil, Fortaleza, CE, Brasil

^cUniversidade Federal do Ceará – UFC, Programa de Pós-graduação em Engenharia de Transportes, Departamento de Engenharia de Transportes, Fortaleza, CE, Brasil

^dUniversidade de Lisboa, Instituto Superior Técnico, Civil Engineering Research and Innovation for Sustainability – CERIS, Lisboa, Portugal

Received February 06, 2023

Revised August 01, 2023

Accepted September 26, 2023

Corrected 27 March 2024

Abstract: The growth of cities affects their permeable surface, which can unbalance hydrological cycles. The pervious concrete can be a viable solution to combat urban environmental impacts in this subject. This type of concrete can be told apart by the presence of interconnected pores and its drainage capacity. This paper aims to analyze the relationship between aggregate shape, mechanical resistance, and permeability of pervious concrete slabs containing steel slag. A Digital Image Processing (DIP) based method was used to measure aggregate shape properties. Three different mixes, using three types of coarse aggregate (gravel 12.5 mm, gravel 9.5 mm, and coarse steel slag), and a type of fine aggregate (fine slag) were tested, and flexural strength, flow, and permeability coefficients were obtained for the slabs. Results showed the potential of using steel slag, with higher flexural strength results (4.61 MPa). Indications of the relationship between aggregate shape parameters and slab properties were determined, with more polished, more angular, and more spherical material resulting in higher flexural strength values and lower permeability coefficient. The inverse relationship between the slabs' permeability parameters and flexural strength was observed.

Keywords: aggregate shape, mechanical resistance, permeability, pervious concrete.

Resumo: O crescimento das cidades afeta a sua superfície permeável, o que pode desequilibrar os ciclos hidrológicos. O concreto permeável pode ser uma solução viável para combater os impactos ambientais urbanos relacionados a esses problemas. Este tipo de concreto é caracterizado pela presença de poros interligados e pela sua alta capacidade de drenagem. Esta pesquisa visa analisar a relação entre a forma dos agregados, a resistência mecânica e a permeabilidade de placas de concreto permeáveis contendo escórias de aciaria. Utilizou-se um método baseado no Processamento Digital de Imagem (PDI) para avaliar as propriedades da forma do agregado. Foram testadas três misturas diferentes, utilizando três tipos de agregados graúdos (brita 12,5 mm, brita 9,5 mm, e escória grossa), e um tipo de agregado fino (escória fina), e foram obtidos valores resistência à flexão, fluxo e coeficientes de permeabilidade para as placas. Os resultados mostraram o potencial da utilização de escória de aciaria, com resultados de resistência à flexão elevados (4,61 MPa). Determinaram-se relações entre parâmetros de forma agregados e propriedades das placas, com um agregado mais polido, mais angular e mais esférico, resultando em valores de resistência à flexão mais

Corresponding author: Ivo de Castro Carvalho. E-mail: ivodecastro@alu.ufc.br

Financial support: Coordination of Superior Level Staff Improvement (CAPES – Finance Code 001).

Conflict of interest: Nothing to declare.

Data Availability: The data that support the findings of this study are available from the corresponding author, ICC, upon reasonable request.

This document has an erratum: <https://doi.org/10.1590/S1983-41952024000500011>



This is an Open Access article distributed under the terms of the Creative Commons Attribution License, which permits unrestricted use, distribution, and reproduction in any medium, provided the original work is properly cited.

elevados e coeficiente de permeabilidade mais baixos. Observou-se uma relação inversa entre os parâmetros de permeabilidade das lajes e a resistência à flexão.

Palavras-chave: forma de agregados, resistência mecânica, permeabilidade, concreto permeável.

How to cite: H. W. Pimentel, I. C. Carvalho, W. B. C. Silva, A. R. Chaves, and L. F. A. L. Babadopulos, "Relationship between the performance of pervious concrete slabs, with steel slag, and the shape properties of coarse aggregates," *Rev. IBRACON Estrut. Mater.*, vol. 17, no. 5, e17501, 2024, <https://doi.org/10.1590/S1983-41952024000500001>

1. INTRODUCTION

Pervious concrete shows a small to zero amount of fine aggregate, which provides a greater porosity for this mixture (15%–35%) [1]–[6]. Then, because of the interconnected internal pores that allow water and air to pass quickly, the pervious concrete shows a drainage potential, being useful in parking lots, roads with low traffic, and pedestrian sidewalks for flood control. Also, this mixture provides sound absorption, noise reduction, and lower heat island effects [6]–[11].

The exponential increase in world population affects the surface areas, mainly in urban areas, due to replacing vegetation with low-permeability materials, which generate more significant flooding and imbalances in hydrological cycles. However, these urban environmental impacts can be reduced using pervious concrete slabs [11]–[13].

The main properties of pervious concrete slabs are related to their permeability coefficient, with an acceptable limit value of at least 1.0 mm/s according to the Brazilian standard ABNT NBR 16416:2015 [14]. Flexural strength should be greater than 2.0 MPa [14], and Strieder et al. [12] obtained flexural strength results between 1.83 MPa and 2.76 MPa for pervious concrete.

Alternative aggregate can be used in concrete for sustainable pervious slabs, using waste and reducing the negative impact of the disposal of these materials, such as Baosteel slag short flow (BSSF), a by-product of the steel industry. The feasibility of this by-product as aggregate in pervious concrete was studied [15]–[18]. Furthermore, the slabs with steel slag could present superior flexural strength results, with an increase ranging from 20%–25%, and better permeability when compared to slabs with natural aggregate [19]. Another satisfactory experiment of using steel slag in pervious concrete was the reduction of the interfacial transition zone of concrete due to the greater hydration of cementitious materials on the slag surface [17].

Steel production in Brazil is relevant, with 34.4 million tons produced in 2017, occupying the 9th place in world production. This production generates about 5 tons of steel slag annually without a defined destination [20]. In Ceará, the local industry Steel Company of Pecem (CSP) produced 2.8 million tons of steel in 2021, which generated approximately 700 thousand tons of slag [21]. Also, this amount of steel slag can cause several pollution-related problems that impact the environment. Therefore, using steel slag as an alternative aggregate is encouraged to reduce the inadequate disposal of this by-product.

The type of material, size, and shape of aggregate directly influence the pervious concrete's properties and performance, affecting its mechanical characteristics, permeability, and durability [22]–[24]. Researchers concluded the existence of strong correlations between the variation of aggregate shape parameters and concrete properties such as flexural strength, compressive strength, permeability, and void percentage [24]–[27]. These parameters can be determined by a Digital Image Processing (DIP) based method using the Aggregate Image Measurement System 2 (AIMS 2) equipment. The outputs for aggregate shape analysis are the Form2D, based on particle radius and angles (fine aggregates only), texture, angularity, and sphericity of particle (coarse aggregate) [25], [28], [29]. However, the coarse aggregate's texture, angularity, and sphericity effects on the mechanical performance and permeability of pervious slabs are not fully known.

Then, this paper aims to analyze the relationship between the shape properties of coarse aggregate and the variation of mechanical and permeability characteristics of pervious concrete slabs, including an evaluation with BSSF steel slag. To this end, pervious concrete slabs were manufactured to be suitable for use in permeable pavements, where each slab is applied separately to build the pavement. In addition, this paper aims to validate such use of waste materials.

2. EXPERIMENTAL PROGRAM

This section first presents the materials used in the investigation (section 2.1). Afterward, the three main methodological steps follow for the investigation of the aggregate shape's effects on the mechanical and permeability characteristics of pervious concrete: (i) aggregate characterization with DIP (section 2.2); (ii) concrete mix and tests on fresh and hardened concrete slabs (section 2.3); and (iii) correlation between shape properties and slab characteristics (section 2.4).

2.1. Materials

Natural and alternative aggregate sources were used. The natural aggregates were 12.5 mm phonolite and 9.5 mm granite gravel. The alternative material consisted of BSSF steel slag, with an original nominal maximum size (NMS) equal to 9.5 mm (9.5 mm steel slag). However, a particle size separation of this waste was performed by using the 2.4 mm sieve (coarse slag > 2.4 mm and fine slag < 2.4 mm). This sieve opening was chosen to use the fine slag as fine aggregate for the three concrete mixes in this research and to approximate the granulometric distribution of the coarse slag (cf. Table 1) with the other two coarse aggregates applied for the concrete mixtures (9.5 mm and 12.5 mm gravels). Furthermore, for the slag, it was possible to obtain equivalent amounts of material larger (= 53% of total mass) and smaller (= 47% of total mass) than 2.4 mm. This was useful for obtaining sufficient fine and coarse slag for the respective concrete dosages used in the drainage slabs (see section 2.3). The aggregates were characterized according to Brazilian Technical Standards Association (ABNT) and American Society for Testing and Materials (ASTM) standards. High-early-strength Portland Cement (ASTM type III and ABNT CP V-ARI) and water from the public distribution network were also used. The visual aspect of the cited materials can be observed in Figure 1.

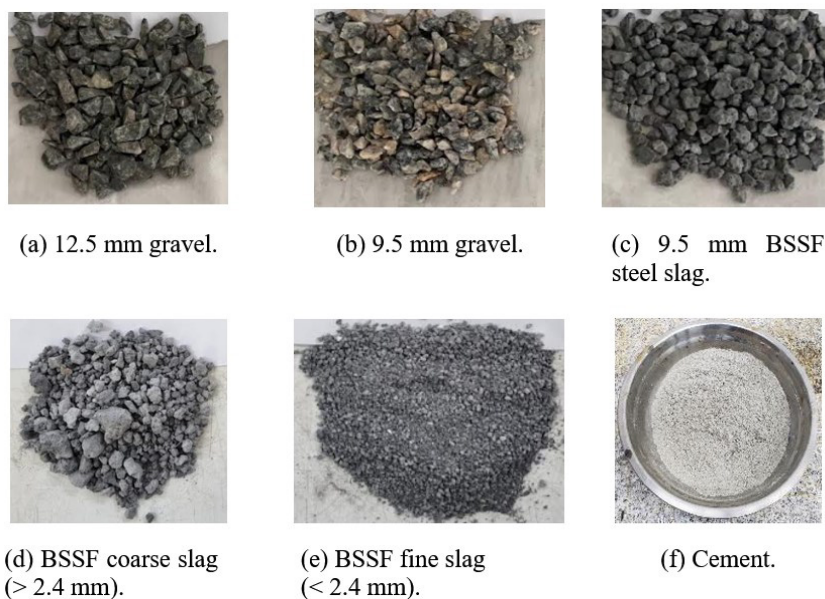


Figure 1. The visual aspect of the materials.

To characterize natural and alternative aggregate, ABNT and ASTM standards were used. The tests performed were: granulometric distribution (NBR 17054:2022 [30] and ASTM C136/C136M-19 [31]), density (ASTM C127-15 [32], ASTM C128-15 [33], ASTM C188-17 [34], NBR 16605:2017 [35], NBR 16916:2021 [36] and NBR 16917:2021 [37]), unit weight, and void content (ASTM C29/C29M-17a [38] and NBR 16972:2021 [39]). The void content was calculated by Equation 1, using the density (specific gravity) and the unit weight. It corresponds to the void content of a dry-rodded sample (in between particles) and not the porosity of a single particle.

$$\text{Void Content} = \frac{\text{Density} - \text{Unit Weight}}{\text{Density}} \quad (1)$$

The granulometric distribution of the materials is shown in Table 1. Furthermore, an analysis of the absolute difference between the accumulated retained percentages on each sieve for the 9.5 mm steel slag and for the coarse slag, compared to the other coarse aggregates, was made in Table 2. Table 2 shows a decrease in the absolute difference of the accumulated retained percentages from 23.44% (average value for the 9.5 mm steel slag) to 13.15% (average value for the coarse slag), which suggests a much better approximation between coarse aggregate gradations after the separation of the 9.5 mm steel slag in coarse and fine slag. The results of the other tests are inserted in Table 3.

Table 1. Aggregates granulometric distribution.

| Sieve (mm) | Accumulated retained percentage (%) | | | | |
|------------|-------------------------------------|-------------|-----------|----------------|---------------|
| | 9.5 mm steel slag | Coarse slag | Fine slag | 12.5 mm gravel | 9.5 mm gravel |
| 19 | 0.00 | 0.00 | 0.00 | 0.00 | 0.00 |
| 12.5 | 2.40 | 4.50 | 0.00 | 2.90 | 0.00 |
| 9.5 | 3.61 | 6.75 | 0.00 | 25.29 | 3.80 |
| 6.3 | 10.32 | 19.32 | 0.00 | 76.69 | 56.12 |
| 4.75 | 18.34 | 34.33 | 0.00 | 92.41 | 86.40 |
| 2.4 | 53.41 | 100.00 | 0.00 | 99.47 | 99.75 |
| 1.2 | 83.37 | 100.00 | 64.30 | 99.97 | 99.75 |
| 0.6 | 94.89 | 100.00 | 89.03 | 99.98 | 99.75 |
| 0.3 | 98.30 | 100.00 | 96.34 | 99.99 | 99.75 |
| 0.15 | 99.20 | 100.00 | 98.28 | 100.00 | 99.75 |
| Pan | 100.00 | 100.00 | 100.00 | 100.00 | 100.00 |

Table 2. Approximation between the granulometric distribution of natural and alternative aggregates.

| Sieve (mm) | 9.5 mm steel slag | | Coarse slag | |
|---|---------------------------------------|--------------------------------------|---|--------------------------------------|
| | Δ A.R. (%) from 12.5 mm gravel | Δ A.R. (%) from 9.5 mm gravel | Δ A.R. (%) from 12.5 mm gravel | Δ A.R. (%) from 9.5 mm gravel |
| 12.5 | 0.50 | 2.40 | 1.60 | 4.50 |
| 9.5 | 21.68 | 0.19 | 18.53 | 2.95 |
| 6.3 | 69.37 | 45.80 | 60.37 | 36.80 |
| 4.75 | 74.07 | 68.06 | 58.07 | 52.07 |
| 2.4 | 46.06 | 46.34 | 0.53 | 0.25 |
| 1.2 | 16.60 | 16.38 | 0.03 | 0.25 |
| 0.6 | 5.09 | 4.86 | 0.02 | 0.25 |
| 0.3 | 1.69 | 1.45 | 0.01 | 0.25 |
| 0.15 | 0.80 | 0.55 | 0.00 | 0.25 |
| Δ A.R. (%) average value = 23.44 | | | Δ A.R. (%) average value = 13.15 | |

Note: Δ A.R. (%) means the absolute difference between the accumulated retained values of each sieve for the coarse aggregates.

Table 3. Aggregates and cement characteristics.

| Materials | NMS (mm) | Fineness modulus | Density (g/cm ³) | Unit weight (kg/m ³) | Void content (%) |
|---|----------|------------------|------------------------------|----------------------------------|------------------|
| 12.5 mm gravel | 12.5 | 6.17 | 2.51 | 1,370.54 | 45.4 |
| 9.5 mm gravel | 9.5 | 5.89 | 2.55 | 1,380.00 | 45.9 |
| 9.5 mm steel slag (before the separation) | 9.5 | 4.51 | 3.61 | – | – |
| Coarse slag | 12.5 | 5.41 | 3.61 | 1,770.00 | 51.0 |
| Fine slag | 2.4 | 3.48 | 3.61 | 1,850.00 | 48.8 |
| Cement | – | – | 3.13 | – | – |

According to Table 3, it should be noted that the fine and coarse slags have the highest values of density (3.61 g/cm³) and unit weight (1,770.00 kg/m³ for coarse slag and 1,850.00 kg/m³ for fine slag), which makes sense, to the fact that they are by-products coming from steel. In addition, the 12.5 mm gravel has the highest fineness modulus (6.17) and the lowest void content between grains, with a value of 45.4%. Despite this, slabs with 12.5 mm gravel would not necessarily have a lower void content. This is because granular packing can change this parameter, and it is crucial for the performance of boards that are not affected only by the void content of the aggregates.

2.2. Aggregate characterization with AIMS 2

12.5 mm and 9.5 mm gravels and coarse slag were analyzed by the DIP in the AIMS 2 equipment according to the National Department of Transport Infrastructure (DNIT) and American Association of State Highway and Transportation Officials (AASHTO) standards DNIT-ME 432:2020 [40] and AASHTO TP 381:2022 [41]. At the same time, the remaining aggregates were not tested since they were used in all mixes. With the analyses, average and percentage values were provided for each classification zone of the following shape properties: angularity, sphericity, and texture. Figure 2 shows the AIMS 2 equipment that performs DIP.

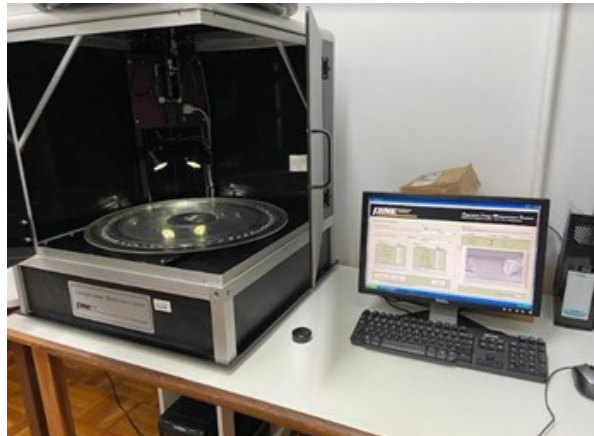


Figure 2. AIMS 2 equipment and digital image processing results.

In this research, the aggregate shape classification system proposed by Ibiapina [42] was adopted regarding the shape properties of the AIMS 2 equipment. It was decided to use this classification due to the citation in the standard DNIT-ME 432:2020 [40] and the fact that the materials used in the referred research are from Brazil. Table 4 presents the aggregate shape classification system proposed by Ibiapina [42].

Table 4. Aggregate shape classification system for AIMS 2 equipment.

| Shape properties | Limit [42] | | | | |
|------------------|----------------|----------------|---------------------|--------------------|----------------|
| Angularity | < 1,260 | 1,260 – 4,080 | 4,080 – 7,180 | > 7,180 | – |
| | Rounded | Sub-rounded | Sub-angular | Angular | |
| Sphericity | < 0.5 | 0.5 – 0.7 | 0.7 – 0.9 | > 0.9 | – |
| | Flat elongated | Low sphericity | Moderate sphericity | High sphericity | |
| Texture | < 260 | 260 – 440 | 440 – 600 | 600 – 825 | > 825 |
| | Polished | Smooth | Low roughness | Moderate roughness | High roughness |

Table 5 presents the classification results of the shape properties for the coarse aggregates (coarse slag, 12.5 mm and 9.5 mm gravels). For this process, the highest percentage observed among all the fractions was used, according to Ibiapina [42]. Figure 3 shows image processing results for the 9.5 mm and 12.5 mm gravels and the coarse slag.

Table 5. Aggregate shape classification results.

| Aggregates | Shape properties | Highest percentage observed (zone limits) | Classification results |
|----------------|------------------|---|------------------------|
| 12.5 mm gravel | Angularity | 88.7% (1,260.0 – 4,080.0) | Sub-rounded |
| | Sphericity | 57.7% (0.5 – 0.7) | Low sphericity |
| | Texture | 62.7% (260.0 – 440.0) | Smooth |
| Coarse slag | Angularity | 62.0% (4,080.0 – 7,180.0) | Sub-angular |
| | Sphericity | 86.0% (0.7 – 0.9) | Moderate sphericity |
| | Texture | 64.0% (260.0 – 440.0) | Smooth |
| 9.5 mm gravel | Angularity | 94.0% (1,260.0 – 4,080.0) | Sub-rounded |
| | Sphericity | 56.6% (0.5 – 0.7) | Low sphericity |
| | Texture | 56.6% (< 260.0) | Polished |

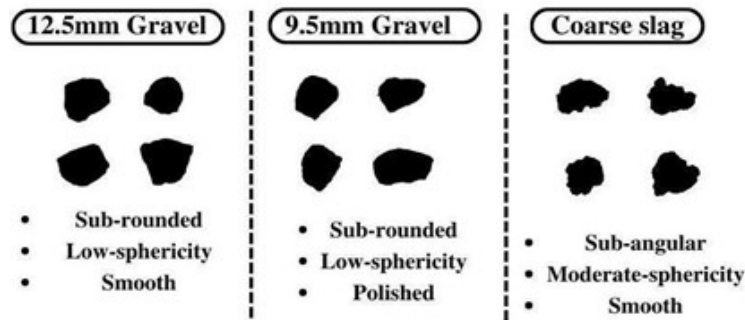


Figure 3. Digital Image Processing results for all coarse aggregates.

Analyzing the texture, the natural aggregates 12.5 mm and 9.5 gravels were classified as smooth and polished, respectively. This may be related to the origin of the rock, in which the 12.5 mm and 9.5 mm gravels come from phonolite and granitic materials, respectively. According to Al-Rousan [43], as the texture is related to the irregularities on the aggregate surface, the phonolite rock can be rougher than the granite in the Metropolitan Region of Fortaleza.

Also, the alternative aggregate coarse slag presented variations in the three shape properties compared to 9.5 mm gravel. Besides the origin of these materials being different, where the slag is a steel by-product, the production process of the aggregates is also quite different. Then, due to how the natural aggregate is crushed, the changes in direction along the contour of the particles may have caused the 9.5 mm gravel to present less angularity than the coarse slag obtained after foaming processes that leave very irregular contours when air escapes.

2.3. Concrete mix and tests on fresh and hardened concrete slabs

Materials batches were made for the production of pervious concrete. Adaptations were made to a reference mix used by a company specialized in the fabrication of slabs with dimensions of 50 cm × 50 cm × 6 cm (length × width × thickness) for permeable pavements and sidewalks in the region of the study. This reference mix aims to provide pervious concrete with a flexural strength of 2 MPa at 28 days, which follows the specifications of the standard ABNT NBR 16416:2015 [14].

Then, three mixes were designed, keeping the volumes of materials constant, with fine slag as fine aggregate in all mixes. In other words, although mass composition differs, the idea in the research is to maintain gradation amongst all concrete mixes and vary only the coarse aggregate (consequently its shape). The coarse slag and the 12.5 mm and 9.5 mm gravels were applied as coarse aggregates in one mixture each. To determine the consumption in kg/m³ of concrete components, Equations 2 and 3 [44] were used.

$$C = (1000 - 10 \times void) / (1/\gamma_c + a/\gamma_a + p/\gamma_p + w/c) \tag{2}$$

$$C_{mat} = C \times P_{mat} \tag{3}$$

where C = The cement consumption per cubic meter of concrete densified (kg/m³); C_{mat} = the consumption of the concrete component materials (kg/m³); $void$ = the void content of the concrete per cubic meter (%); γ_c , γ_a and γ_p = the density of cement, fine and coarse aggregate, respectively (kg/dm³); a and p = the ratio of fine and coarse aggregate, as a function of cement, in the mix, respectively; w/c = the water/cement ratio and P_{mat} = the ratio of the component material of the concrete, in the function of the cement, in the mix.

The void content of concrete in the fresh state, the “*void*” parameter in Equation 2, was determined according to ABNT NBR 9833:2008 [45] and ASTM C1688/1688M:14a [46]. However, instead of using a cylindrical container, which should be filled with fresh concrete, it was chosen to analyze two slabs freshly produced by the vibro-press machine (see Figure 4) for each of the three mixes. Then, the mass and volume of the slabs were determined to obtain the concrete’s average unit weight (property necessary to calculate the void content). This procedure was adopted due to the inability to simulate, through manual or vibrated compaction, the compaction energy provided by the vibro-press machine. With these explanations, the mixtures tested are presented in Table 6.

Table 6. Consumption of the materials for the three concrete mixes used to fabricate the tested pervious concrete slabs.

| Concrete mixes | Unit weight (kg/m ³) | Void content (%) | Consumption (kg/m ³) | | | | Materials proportions by weight |
|---------------------------------------|----------------------------------|------------------|----------------------------------|--------------------|----------------------|-------------|---------------------------------|
| | | | Cement | Fine aggregate (a) | Coarse aggregate (b) | Water (w/c) | 1:a:b:w/c |
| Mix with fine slag and 12.5 mm gravel | 1,575.50 | 37.38 | 329.89 | 330.41 | 807.23 | 107.92 | 1:1.00:2.45:0.33 |
| Mix with fine and coarse slag | 1,935.90 | 36.41 | 329.34 | 329.86 | 1,158.14 | 118.56 | 1:1.00:3.52:0.36 |
| Mix with fine slag and 9.5 mm gravel | 1,785.35 | 29.95 | 372.19 | 372.78 | 924.52 | 115.79 | 1:1.00:2.48:0.31 |

The mix with coarse and fine slag presented the highest average bulk density (1,935.90 kg/m³), which is consistent with the results of Table 3 due to the use of the by-product that showed the highest density value (3.61 g/cm³). Also, the mixture with fine slag and 12.5 mm gravel presented the highest void content (37.38%). However, the mix with fine slag and 9.5 mm gravel had the lowest void content (29.95%), showing that the incorporated air does not depend only on the voids generated by each aggregate. This difference between mixes is also impacted by the granular packing, a parameter influenced by the aggregate shape. Finally, as the three mixtures presented different void contents, cement and other components' consumptions per 1 m³ of each composition were determined using Equations 2 and 3 [44].

The slabs were manufactured in a VP50 model from the TPrex brand vibro-press machine. Initially, slabs with dimensions 50 cm × 50 cm × 6 cm (length × width × thickness) were produced. However, each of these units was cut into four smaller slabs of dimensions 25 cm × 25 cm × 6 cm (length × width × thickness) because it was necessary samples for the tests at 7 and 28 days. In addition, the shape factor of these new slabs was approximately 4.17 (25 cm/6 cm = 4.17), which was following the specification of the standard ABNT NBR 16416:2015 [14]. The procedures are shown in Figure 4. The slabs were produced to be in the conditions for application in permeable pavements after a few days of production. The product manufactured with this machine for industrial purposes represents the final condition for pavement application.

The slabs were tested in the hardened state at 7 and 28 days. The performed tests were visual inspection, three-point flexural strength [14], [47], permeability coefficient [14], [48], and flow coefficient (with the methodology described in more detail afterward). The two last tests are presented in Figure 5.

Based on the standard NBR 16416:2015 [14], as the final concrete slabs had a shape factor of 4.17 (slightly higher than the minimum value of 4 to be classified as slabs, according to [14]), the flexural test was used. The flexural strength was obtained from the three-point flexural strength test performed on the pervious concrete slab, according to the standard NBR 15805:2015 [47], with the application of the load in the center of the upper surface of the slab.

About the permeability coefficient test, a sealing ring attached to the slabs was used, with caulk paste, to prevent water leakage. A flow was promoted from spilling 3,600 ± 50 g of water, keeping the water level in the ring at approximately 10 mm high. The time for the complete passage of the water through the permeable slab was determined, and an expression was used to calculate the permeability coefficient. Equation 4 (ABNT NBR 16416:2015 [14] and ASTM C1701/C1701M-17a [48]) shows how to calculate the permeability coefficient from the test results. This test was chosen based on the Brazilian standard ABNT NBR 16416:2015 [14], which determines this test as viable for in-situ and laboratory application.

$$k = [C \times m / (d^2 \times t)] / 3600 \tag{4}$$

where *k* is the permeability coefficient of permeable concrete slabs (mm/s); *C* is the conversion factor, with a value equal to 4,583,666,000; *m* is the mass of infiltrated water (kg); *d* is the internal diameter of the water percolation ring (mm) and *t* is the time needed for all the water to percolate (s).

The conversion factor “*C*” has units of (mm³.s)/(kg. h) and is needed to convert the parameters *m*, *d*, and *t* to the permeability coefficient *k* in mm/h, based on the standard ASTM C1701/C1701M:17a [48].



(a) Overview of the vibro-press machine.



(b) Vibro-press machine in operation.



(c) Initial concrete slabs (50 cm x 50 cm x 6 cm).



(d) Final concrete slabs (25 cm x 25 cm x 6 cm) after cut.

Figure 4. Pervious concrete slab production.



(a) Permeability coefficient test



(b) Flow coefficient test.

Figure 5. Pervious concrete slab permeability tests

Regarding the flow coefficient methodology, a water flow of approximately $47 \text{ cm}^3/\text{s}$, adopted by the authors, was applied for 60 seconds to an 18-liter bucket with no obstacle, with a total mass of water of about 2,820 g. The test was performed with a water flow rate experimentally determined to be low enough not to cause a flow that would make the water escape from the top of the slab and fall into the bucket. Besides, it was considered a flow to generate a uniform water distribution on the slab surface. Then, for each mix, three slabs were positioned, one at a time, on top of the same bucket, as shown in Figure 5b, and for 60 seconds, the same flow rate of $47 \text{ cm}^3/\text{s}$ was applied. Then, the mass of water in the container was determined, and it was possible to calculate the percentage, concerning the initial amount of 2,820 g, of passed water. This test aimed to determine a parameter (%) that indicated the slab's draining capacity through the relationship between the volume of water that passed through the slab and the volume applied. Finally, the flow coefficient was the average percentage for the three concrete mixes.

2.4. Analysis of relationships between aggregate shape and pervious concrete properties

It was decided to establish relationships between the average values of the coarse aggregates' shape properties (angularity, sphericity, and texture) and the pervious concrete slabs' characteristics (flexural strength, permeability coefficient, and flow coefficient). Also, it was attempted to relate, in the same graph, only the slab's characteristics cited above, including the flow coefficient. Then, Table 7 follows with more detailed information about the proposed possible relationships to be investigated (the symbols "O" and "X" refer to the presence and non-presence, respectively, of a property or characteristic in the tested relationship) and corresponding requirements to allow comparison without having multiple effects on the same relationship.

"Relationship A" determined the impact of the material's surface texture property since it is present in mixtures with aggregates in the same angularity and sphericity classification range. Then, it isolates the surface texture as the only variable, making it possible to determine how much the change in texture of the aggregates impacts the flexural strength and the coefficient of permeability of the pervious concrete slabs.

"Relationship B" determined the impact of the material's angularity and sphericity properties on the flexural strength and permeability coefficient of pervious concrete slabs. This impact was determined since it was a relationship that referred only to slabs with aggregates with the same surface texture classification range, disregarding this as a variable in this proposed relationship.

Finally, "Relationship C" analyzed any possible relationship between the slab's three properties analyzed. Differently from Relationships A and B, this relationship did not consider the shape properties of the aggregates. It was a relationship that studied only the mechanical and permeability properties of the slabs, aiming to relate the flexural strength, the permeability coefficient, and the flow coefficient among themselves.

The 12.5 mm and 9.5 mm gravels were classified in the same angularity zone (sub-rounded) and sphericity zone (low sphericity). Then, the two mixtures with these coarse aggregates were analyzed according to Relationship A (impact of the aggregate's surface texture on the slab's flexural strength and permeability coefficient), as shown in Table 7. The 12.5 mm gravel and the coarse slag were situated in the same classification zone for texture (smooth). This means that the two concrete mixes with these coarse aggregates were evaluated according to Relationship B (impact of the aggregate's angularity and sphericity in combination on the slab's flexural strength properties and coefficient of permeability). Finally, Relationship C studied the impact between the slab's three properties (flexural strength, permeability coefficient, and flow coefficient) among themselves for all mixtures.

Table 7. Relationships between coarse aggregates' shape properties and drainage slabs' characteristics.

| Properties | Relationships between properties | | | Mixes in each relationship | | |
|-----------------|----------------------------------|---|---|----------------------------|---|--|
| | A | B | C | A | B | C |
| Aggregate shape | Angularity | X | O | X | 1. Mix with fine slag and 9.5 mm gravel 1. Mix with fine slag and 12.5 mm gravel | 1. Mix with fine slag and 9.5 mm gravel |
| | Sphericity | X | O | X | | 2. Mix with fine slag and 12.5 mm gravel |
| | Texture | O | X | X | | |
| Concrete slab | Flexural strength | O | O | O | 2. Mix with fine slag and 12.5 mm gravel 2. Mix with fine slag and coarse slag | 3. Mix with fine slag and coarse slag |
| | Permeability coefficient | O | O | O | | |
| | Flow coefficient | X | X | O | | |

Note: O aggregate or concrete slab's properties present in a relationship; X aggregate or concrete slab's properties not present in a relationship.

3. RESULTS AND DISCUSSION

3.1. Hardened state characterization on pervious concrete slabs

Regarding the visual inspection of the concrete slabs for the three mixes, Figure 6 shows the three types of concrete slabs. Furthermore, Figure 7 shows the flexural strength, permeability, and flow coefficient results for the three concrete mixes, with the standard deviation bars for a better data distribution understanding.

According to Figures 6 and 7, the slabs with fine slag and 12.5 mm gravel presented lower compactness due to the more significant apparent voids on the concrete surface. This key factor contributed to the mix presenting the highest flow (98.12% and 97.36% at 7 and 28 days, respectively) and permeability (2.372 mm/s and 2.366 mm/s at 7 and 28 days, respectively) coefficients. Then, the material type in this mix may have contributed to the mixture being the least compact after the vibration applied by the vibro-press machine. In contrast to this situation, the slabs with coarse and fine slag, according to Figure 6, appeared to be the most compact. This is evidenced in Figures 7a and b by this concrete providing the lowest flow (96.28% and 92.65% at 7 and 28 days, respectively) and permeability (1.195 mm/s and 1.157 mm/s at 7 and 28 days, respectively) coefficients. Then, the packing caused by using coarse and fine slags together, besides being materials of the same origin, can be related to the greater compactness presented by the slabs. Also, the aggregate shape properties can be a key factor in the pervious slab's performance.

In Figure 7b, all slabs were approved concerning the permeability coefficient limit values in standards, such as ABNT NBR 16416:2015 [14] (minimum of 1.0 mm/s) and CJJ/T 135-2009 [49] (minimum of 0.5 mm/s). However, analyzing the range of values recommended by the Portland Cement Association [50], where the permeability coefficient must be between 1.3 mm/s to 12.2 mm/s, only the slabs with fine and coarse slag showed values below the range (1.195 mm/s and 1.157 mm/s at 7 days and 28 days, respectively). The significant value of 12.2 mm/s tolerated by the Portland Cement Association [50] may be related to the maximum flexural strength value of 3.8 MPa. The reason is that slabs with high flexural strength may have a dense structure, impairing the concrete permeability, which is the most important characteristic considered by the Portland Cement Association [50]. About the flow coefficient, all values were higher than 90%, showing the permeability of all slabs according to pervious concrete slabs manufacturers [51], [52].

Regarding the flexural strength in Figure 7c, all the mixes were approved in the standard ABNT NBR 16416:2015 [14] (minimum of 2.0 MPa at 28 days). It should also be noted that the slabs with coarse and fine slags were approved in Brazilian, Chinese, and American standards [14], [49], [50], besides presenting the highest average value of flexural strength (3.83 MPa and 4.61 MPa at 7 and 28 days, respectively). Then, using these alternative materials may be useful for concrete slab production for permeable pavements, with greater longevity, given the stresses arising from pedestrian traffic. Also, from the environmental point of view, it is essential to use by-products that provide a valuable purpose, such as paving works.

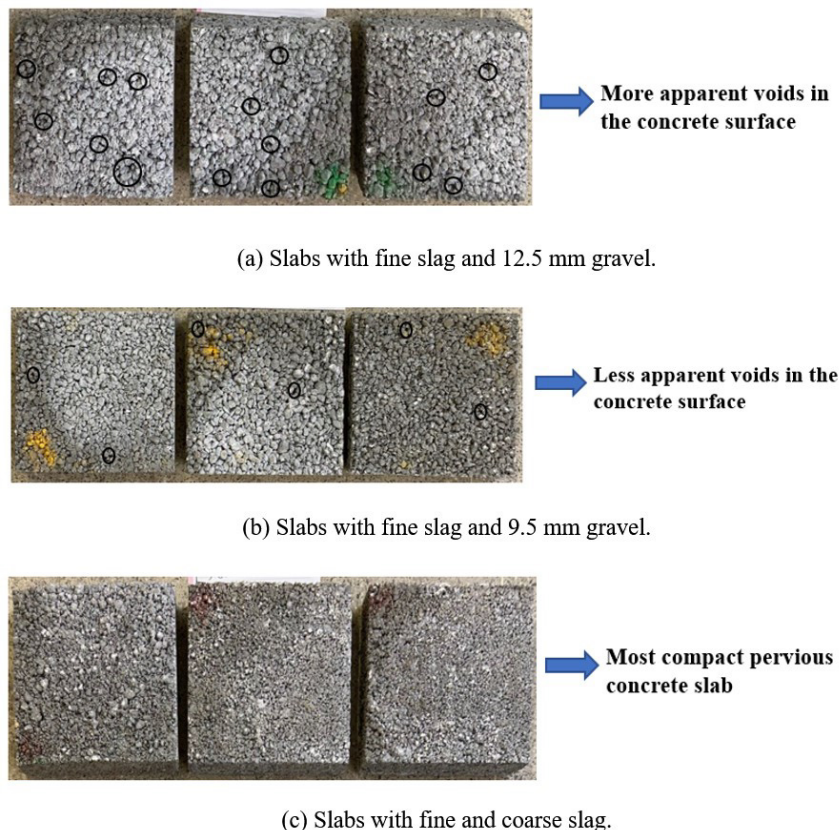
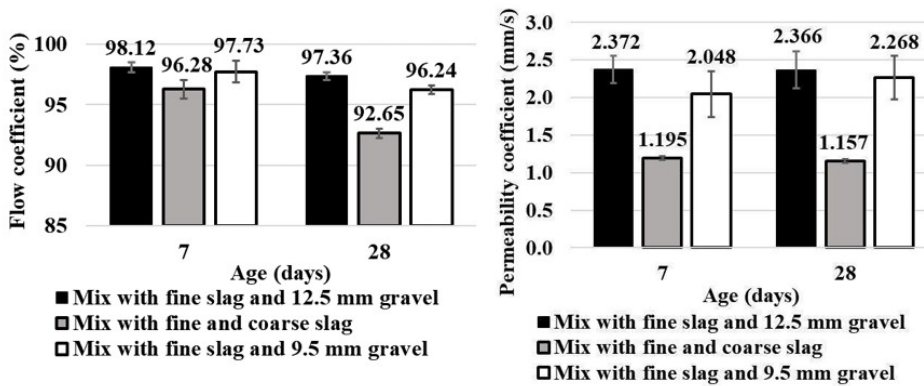
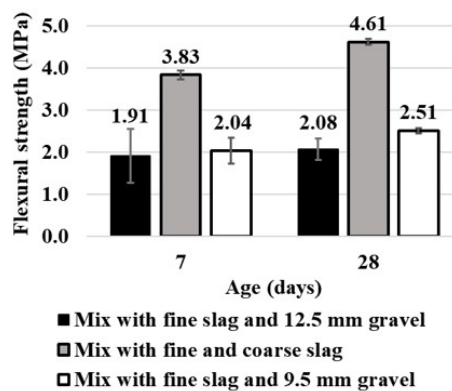


Figure 6. Pervious concrete slab visual inspection.



(a) Flow coefficient.

(b) Permeability coefficient.



(c) Flexural strength.

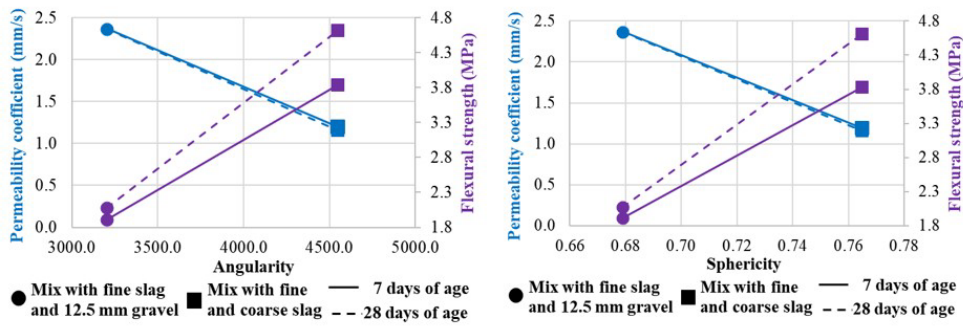
Figure 7. Result tests on concrete slabs.

3.2. Relationships between the aggregate shape properties and the pervious concrete slab characteristics

Figure 8 shows the results from Relationships A and B (see Table 7). Also, Figure 9 presents a two-dimensional graph establishing Relationship C (see Table 7) between the slabs' characteristics.

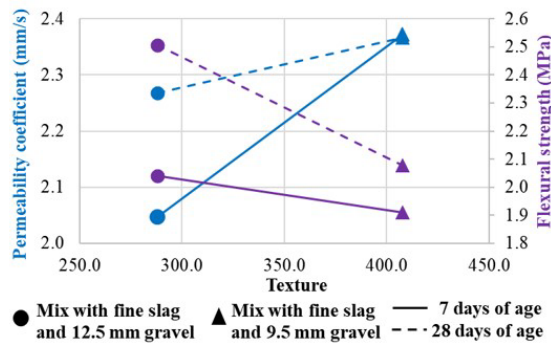
Analyzing Figure 8c, it seems that the increase in flexural strength and the decrease in the permeability coefficient of the slabs may be related to the coarse aggregate texture decrease. Also, the increase in flexural strength and the decrease in the slabs' permeability coefficient may be related to the increases in both coarse aggregate angularity and sphericity (Figures 8a and b).

In Figure 8, according to Relationships A and B, the combination of the decrease in texture and the increase in angularity and sphericity of the coarse aggregates generated more significant strengths to the pervious concrete slabs. This observation may be mainly related to the greater interlocking of particles linked to these shape properties. Also, the decrease in coarse aggregate roughness may favor the concrete compactness after the vibration applied by the vibro-press machine. Then, there was an increase in flexural strength and a decrease in the permeability coefficient. To corroborate this discussion, Masad et al. [53], Altuki et al. [25], and Wu et al. [54] stated that mixtures with more angular and rougher aggregates presented a better interlocking between particles, consequently improving the strengths and decreasing the permeability, as observed in the results from this paper. In addition, the same authors indicated that those shape properties were essential to generate friction at the interface between the tire and the pavement. Also, according to Wu et al. [54], the increase in the sphericity of aggregates decreased the number of pores in a pervious concrete mixture, increasing its mechanical strength and decreasing its permeability, converging with the results found in this research.



(a) Result of Relationship B (Part 1).

(b) Result of Relationship B (Part 2).



(c) Result of Relationship A.

Figure 8. Results of Relationships A and B from Table 7.

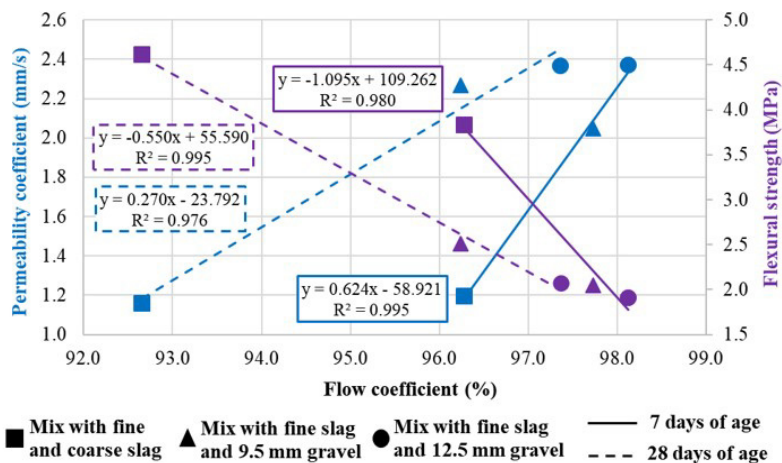


Figure 9. A graphical representation of Relationship C from Table 7.

Regarding Relationship C (see Figure 9), with the increase in the flow coefficient, the permeability coefficient increased, and the flexural strength decreased, being related to the number of interconnected pores in the concrete structure, where not necessarily a slab with a significant volume of voids will be permeable unless pores are connected. Then, the presence of these voids ensured a considerable flow coefficient of the slabs, making them also permeable. However, a very porous structure impaired the mechanical behavior of concrete due to the lack of compactness, which explains this expected decrease in flexural strength as the flow coefficient increases.

In Figure 8, regarding the ages of 7 and 28 days, Relationships A and B showed a similarity of the behavior related to the influence of the shape factors (texture, angularity, and sphericity of coarse aggregate) on the pervious concrete mixtures' flexural strength properties and permeability coefficient. Also, despite the difference in absolute values of strength and permeability coefficient (especially with the increase in strength due to aging), the mixture age did not change the general impact pattern of these properties on the slabs, where it is possible to identify the same type of impact between the aggregates' shape properties the slabs' characteristics. This same behavior for both ages was also observed in Relationship C (see Figure 9).

4. CONCLUSIONS

This paper investigated the shape properties of three different aggregate sources, including BSSF steel slag, and their impact on pervious concrete mechanical and permeability characteristics. With the main results, the leading direct inferences can be as follows:

- All three concrete mixes showed satisfactory permeability coefficients according to Brazilian, American, and Chinese criteria. Also, the slabs with phonolite 12.5 mm gravel presented the highest permeability coefficients, with values of 2.372 mm/s and 2.366 mm/s at 7 days and 28 days, respectively;
- All three concrete mixes showed average flexural strength above the minimum Brazilian standard limit value of 2.0 MPa. Furthermore, the slabs with coarse and fine slags presented the highest average value of flexural strength (3.83 MPa and 4.61 MPa at 7 and 28 days, respectively);
- An inverse correlation was noted between the coarse aggregate's texture and the concrete slab's flexural strength;
- A direct correlation was observed between the coarse aggregate's sphericity and angularity shape variables and the concrete slab's flexural strength;
- A direct correlation was discovered between the coarse aggregate's texture and the concrete slab's permeability coefficient;
- An inverse correlation was detected between the coarse aggregate's sphericity and angularity shape variables and the concrete slab's permeability coefficient.

It is essential to highlight that the analyses performed are still limited due to the small number of concrete mixes produced. However, the observed relationships between aggregate shape and slab properties are per literature for other materials, and then generating a first understanding of the concrete mix aggregate interlocking and properties behavior. Aiming for a more definitive analysis regarding the relationships between aggregate shape and properties of permeable concrete slabs, more concrete mixes should be produced in future research, allowing the development of more complete graphical analyses and more generalizable results.

Finally, this study supports the relationships between the mechanical and permeability properties of the slabs, in which there is a direct influence between the flow coefficient and the interconnected pores of the slabs. A high flow coefficient indicates more significant voids, increasing the permeability coefficient and decreasing the flexural strength.

ACKNOWLEDGEMENTS

The authors acknowledge the support of companies Apodi, StonePlus, Britacet, OCS, and Steel Company of Pecem (CSP) for providing materials and manufacturing the concrete slabs for the research. This study was funded in part by the Coordenação de Aperfeiçoamento de Pessoal de Nível Superior–Brasil (CAPES)–Finance Code 001. The support of the Federal University of Ceará's labs is as well acknowledged, such as the Laboratory of Civil Construction Materials and the Laboratory of Geology.

REFERENCES

- [1] K. S. Elango and V. Revathi, "Fal-G "Binder Pervious Concrete," *Constr. Build. Mater.*, vol. 140, pp. 91–99, 2017, <http://dx.doi.org/10.1016/j.conbuildmat.2017.02.086>.
- [2] S. T. Martins, R. Pieralisi, and F. C. Lofrano, "Framework to characterize nonlinear flow through pervious concrete," *Cement Concr. Res.*, vol. 151, pp. 106633, 2022, <http://dx.doi.org/10.1016/j.cemconres.2021.106633>.
- [3] S. T. Martins, E. M. Bosquesi, J. R. Fabro, and R. Pieralisi, "Characterization of pervious concrete focusing on non-destructive testing," *Rev. IBRACON Estrut. Mater.*, vol. 13, no. 3, pp. 483–500, 2020, <http://dx.doi.org/10.1590/S1983-41952020000300003>.
- [4] S. Juradin, F. Mihanović, N. Ostojić-Škomrlj, and E. Rogošić, "Pervious concrete reinforced with waste cloth strips," *Sustainability*, vol. 14, no. 5, pp. 2723, 2022, <http://dx.doi.org/10.3390/su14052723>.

- [5] T. Hemalatha, N. Ranjit Raj, and R. Gopal, "Pervious concrete for green walls," *J. Archit. Eng.*, vol. 27, no. 4, pp. 06021003, 2021, [http://dx.doi.org/10.1061/\(ASCE\)AE.1943-5568.0000509](http://dx.doi.org/10.1061/(ASCE)AE.1943-5568.0000509).
- [6] W. Xu, B. Chen, X. Chen, and C. Chen, "Influence of aggregate size and notch depth ratio on fracture performance of steel slag pervious concrete," *Constr. Build. Mater.*, vol. 273, pp. 122036, 2021, <http://dx.doi.org/10.1016/j.conbuildmat.2020.122036>.
- [7] J. Cai et al., "Mix design methods for pervious concrete based on the mesostructure: Progress, existing problems and recommendation for future improvement," *Case Stud. Constr. Mater.*, vol. 17, pp. e01253, 2022, <http://dx.doi.org/10.1016/j.cscm.2022.e01253>.
- [8] X. Chen, J. Wang, Y. Ning, R. Zhao, and J. Tong, "Properties and microstructures of steel slag pervious concrete with anticrack additives," *J. Transp. Eng. Part B. Pavements*, vol. 148, no. 2, pp. 04022020, 2022, <http://dx.doi.org/10.1061/JPEODX.0000362>.
- [9] J. Shan, Y. Zhang, S. Wu, Z. Lin, L. Li, and Q. Wu, "Pore characteristics of pervious concrete and their influence on permeability attributes," *Constr. Build. Mater.*, vol. 327, pp. 126874, 2022, <http://dx.doi.org/10.1016/j.conbuildmat.2022.126874>.
- [10] K. Tan, Y. Qin, and J. Wang, "Evaluation of the properties and carbon sequestration potential of biochar-modified pervious concrete," *Constr. Build. Mater.*, vol. 314, pp. 125648, 2022, <http://dx.doi.org/10.1016/j.conbuildmat.2021.125648>.
- [11] B. Debnath and P. Sarkar, "Permeability prediction and pore structure feature of pervious concrete using brick as aggregate," *Constr. Build. Mater.*, vol. 213, pp. 643–651, 2019, <http://dx.doi.org/10.1016/j.conbuildmat.2019.04.099>.
- [12] H. Strieder, V. Dutra, A. Graeff, W. Núñez, and F. Merten, "Performance evaluation of pervious concrete pavements with recycled concrete aggregate," *Constr. Build. Mater.*, vol. 315, pp. 125384, 2022, <http://dx.doi.org/10.1016/j.conbuildmat.2021.125384>.
- [13] F. Merten, V. Dutra, H. Strieder, and A. Graeff, "Clogging and maintenance evaluation of pervious concrete pavements with recycled concrete aggregate," *Constr. Build. Mater.*, vol. 342, pp. 127939, 2022, <http://dx.doi.org/10.1016/j.conbuildmat.2022.127939>.
- [14] Associação Brasileira de Normas Técnicas, *Pervious Concrete Pavements – Requirements and Procedures*, ABNT NBR 16416, 2015.
- [15] L. C. B. Costa, M. A. Nogueira, L. C. Ferreira, F. P. F. Elói, J. M. F. Carvalho, and R. A. F. Peixoto, "Eco-efficient steel slag concretes: an alternative to achieve circular economy," *Rev. IBRACON Estrut. Mater.*, vol. 15, no. 2, pp. e15201, 2022, <http://dx.doi.org/10.1590/S1983-41952022000200001>.
- [16] S. Wang, G. Zhang, B. Wang, and M. Wu, "Mechanical strengths and durability properties of pervious concretes with blended steel slag and natural aggregate," *J. Clean. Prod.*, vol. 271, pp. 122590, 2020, <http://dx.doi.org/10.1016/j.jclepro.2020.122590>.
- [17] X. Chen, G. Wang, Q. Dong, X. Zhao, and Y. Wang, "Microscopic characterizations of pervious concrete using recycled Steel Slag Aggregate," *J. Clean. Prod.*, vol. 254, pp. 120149, 2020, <http://dx.doi.org/10.1016/j.jclepro.2020.120149>.
- [18] L. Lang, H. Duan, and B. Chen, "Properties of pervious concrete made from steel slag and magnesium phosphate cement," *Constr. Build. Mater.*, vol. 209, pp. 95–104, 2019, <http://dx.doi.org/10.1016/j.conbuildmat.2019.03.123>.
- [19] K. Ćosić, L. Korat, V. Ducman, and I. Netinger, "Influence of aggregate type and size on properties of pervious concrete," *Constr. Build. Mater.*, vol. 78, pp. 69–76, 2015, <http://dx.doi.org/10.1016/j.conbuildmat.2014.12.073>.
- [20] F. Amancio, A. Dias, D. Lima, and A. E. Cabral, "Study of the behavior in the fresh and hardened state of mortar with BSSF steel slag," *Rev Mater.*, v. 26, no. 3, pp. e13031, 2021, <https://doi.org/10.1590/S1517-707620210003.13031>.
- [21] Revista Mineração e Sustentabilidade, "CSP reaches records in the production of premium steels," 2022. <https://revistaminerao.com.br/2022/02/09/csp-atinge-recordes-na-producao-de-acos-premium/> (accessed July 8, 2022).
- [22] F. Yu, D. Sun, J. Wang, and M. Hu, "Influence of aggregate size on compressive strength of pervious concrete," *Constr. Build. Mater.*, vol. 209, pp. 463–475, 2019, <http://dx.doi.org/10.1016/j.conbuildmat.2019.03.140>.
- [23] L. G. Li et al., "Effects of aggregate bulking and film thicknesses on water permeability and strength of pervious concrete," *Powder Technol.*, vol. 396, pp. 743–753, 2022, <http://dx.doi.org/10.1016/j.powtec.2021.11.019>.
- [24] L. Shtrepi, A. Astolfi, E. Badino, G. Volpatti, and D. Zampini, "More than just concrete: acoustically efficient porous concrete with different aggregate shape and gradation," *Appl. Sci. (Basel)*, vol. 11, no. 11, pp. 4835, 2021, <http://dx.doi.org/10.3390/app11114835>.
- [25] R. Altuki, M. Ley, D. Cook, M. Gudimentla, and M. Praul, "Increasing sustainable aggregate usage in concrete by quantifying the shape and gradation of manufactured sand," *Constr. Build. Mater.*, vol. 321, pp. 125593, 2022, <http://dx.doi.org/10.1016/j.conbuildmat.2021.125593>.
- [26] Y. Zhou, H. Jin, and B. Wang, "Modeling and mechanical influence of meso-scale concrete considering actual aggregate shapes," *Constr. Build. Mater.*, vol. 228, pp. 116785, 2019, <http://dx.doi.org/10.1016/j.conbuildmat.2019.116785>.
- [27] E. Piotrowska, Y. Malecot, and Y. Ke, "Experimental investigation of the effect of coarse aggregate shape and composition on concrete triaxial behavior," *Mech. Mater.*, vol. 79, pp. 45–57, 2014, <http://dx.doi.org/10.1016/j.mechmat.2014.08.002>.
- [28] L. Diógenes, R. Maia, I. Bessa, V. Castelo Branco, J. Nogueira No., and F. Silva, "The influence of crushing processes and mineralogy of aggregates on their shape properties and susceptibility to degradation," *Constr. Build. Mater.*, vol. 284, pp. 122745, 2021, <http://dx.doi.org/10.1016/j.conbuildmat.2021.122745>.
- [29] D. Ibiapina, L. Diógenes, V. Castelo Branco, S. Freitas, L. Motta, and D. Diógenes, "Statistical analysis of the quality of the measurements of the shape properties of aggregates using the Digital Image Processing (DIP)," *Transportes*, vol. 28, pp. 1-12, 2020, <http://dx.doi.org/10.14295/transportes.v28i1.1865>.

- [30] Associação Brasileira de Normas Técnicas, *Aggregates – Determination of Granulometric Composition – Test Method*, ABNT NBR 17054, 2022.
- [31] American Society for Testing and Materials, *Standard Test Method for Sieve Analysis of Fine and Coarse Aggregates*, ASTM C136/C136M-19, 2019.
- [32] American Society for Testing and Materials, *Standard Test Method for Density, Relative Density (Specific Gravity), and Absorption of Coarse Aggregate*, ASTM C127-15, 2015.
- [33] American Society for Testing and Materials, *Standard Test Method for Relative Density (Specific Gravity) and Absorption of Fine Aggregate*, ASTM C128-15, 2015.
- [34] American Society for Testing and Materials, *Standard Test Method for Density of Hydraulic Cement*, ASTM C188-17, 2017.
- [35] Associação Brasileira de Normas Técnicas, *Portland Cement and Other Powdered Materials – Determination of the Density*, ABNT NBR 16605, 2017.
- [36] Associação Brasileira de Normas Técnicas, *Fine Aggregate – Determination of Density and Water Absorption*, ABNT NBR 16916, 2021.
- [37] Associação Brasileira de Normas Técnicas, *Coarse Aggregate – Determination of Density and Water Absorption*, ABNT NBR 16917, 2021.
- [38] American Society for Testing and Materials, *Standard Test Method for Bulk Density (“Unit Weight”) and Voids in Aggregate*, ASTM C29/C29M-17a, 2017.
- [39] Associação Brasileira de Normas Técnicas, *Aggregates – Determination of the Unit Weight and Air-void Contents*, ABNT NBR 16972, 2021.
- [40] National Transportation Infrastructure Department, *Aggregates – Determination of the Shape Properties by Means of Digital Image Processing (DIP) – Test method*, DNIT-ME 432, 2020.
- [41] American Association of State and Highway Transportation Officials, *Standard Method of Test for Determining Aggregate Shape Properties by Means of Digital Image Analysis*, AASHTO TP 381-22, 2022.
- [42] D. S. Ibiapina, "Proposition of a classification system for the shape properties of aggregates characterized using Digital Image Processing for the selection of Brazilian materials," DSc. thesis, Fed. Univ. Ceara, Fortaleza, Brazil, 2018.
- [43] T. M. Al-Rousan, "Characterization of aggregate shape properties using a computer automated system," Ph.D. thesis, Texas A&M Univ., College Station, USA, 2004.
- [44] P. Helene and P. Terzian, *Concrete Dosage and Control Manual*, 1st ed., Sao Paulo, Brazil: Pini Ltda, 1992.
- [45] Associação Brasileira de Normas Técnicas, *Fresh concrete – Determination of the unit weight, yield and air content by the gravimetric test method*, ABNT NBR 9833, 2008.
- [46] American Society for Testing and Materials, *Standard Test Method for Density and Void Content of Freshly Mixed Pervious Concrete*, ASTM C1688/1688M-14a, 2014.
- [47] Associação Brasileira de Normas Técnicas, *Precast Concrete Paving Slabs on pedestals - Requirements and procedures*, ABNT NBR 15805, 2015.
- [48] American Society for Testing and Materials, *Standard Test Method for Infiltration Rate of In Place Pervious Concrete*, ASTM C1701/C1701M-17a, 2017.
- [49] National Standard of the People’s Republic of China, *Technical Specification for Pervious Cement Concrete Pavement*, CJJ/T 135-2009, 2009.
- [50] P. D. Tennis, M. L. Leming, and D. J. Akers, *Pervious Concrete Pavements*, 1st ed., Skokie, USA: Portland Cement Association, 2004.
- [51] AECweb, "Pisos drenantes Conclave garantem permeabilidade de 90%." <https://www.aecweb.com.br/empresa/conclave-pisos/33004/conteudo/pisos-drenantes-conclave-garantem-permeabilidade-de-90/13652> (accessed Aug 12, 2022)
- [52] AECweb, "Pisos Megadreno têm capacidade drenante superior a 90% e são antiderrapantes." <https://www.aecweb.com.br/empresa/braston/6479/conteudo/pisos-megadreno-tem-capacidade-drenante-superior-a-90-e-sao-antiderrapantes/5030> (accessed Aug 12, 2022).
- [53] E. Masad, D. Little, L. Tashman, S. Saadeh, T. Al-Rousan, and R. Sukhwani, *Evaluation of Aggregate Characteristics Affecting HMA Concrete Performance, Report ICAR 203-1*, College Station, USA: Texas Transportation Institute, 2004.
- [54] S. Wu, Q. Wu, J. Shan, X. Cai, X. Su, and X. Sun, "Effect of morphological characteristics of aggregate on the performance of pervious concrete," *Constr. Build. Mater.*, vol. 367, pp. 130219, 2023, <http://dx.doi.org/10.1016/j.conbuildmat.2022.130219>.

Author contributions: HWP: Conceptualization, Methodology, Validation, Resources. ICC: Conceptualization, Writing - original draft, Investigation. WBCS: Data curation, Formal analysis, Supervision. ARC: Methodology, Visualization, Investigation. LfALB: Writing - review & editing, Supervision, Validation.

Editors: Maurício de Pina Ferreira, Guilherme Aris Parsekian.